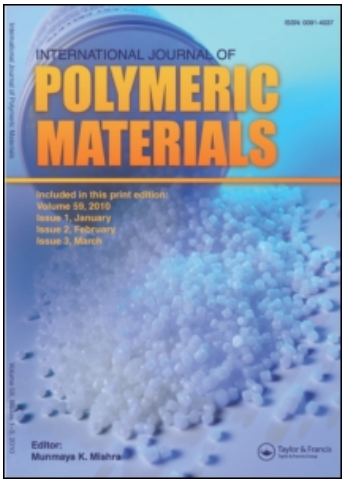

International Journal of Polymeric Materials
Publication details, including instructions for authors and subscription information:
http://www.informaworld.com/smpp/title~content=t713647664

Flame Retardancy of Cellular Polymeric Materials

R. M. Aseeva[a]; G. E. Zaikov[a]
[a] Institute of Chemical Physics, Russian Academy of Sciences, Moscow, Russia

To cite this Article Aseeva, R. M. and Zaikov, G. E.(1996) 'Flame Retardancy of Cellular Polymeric Materials', International Journal of Polymeric Materials, 31: 1, 237 — 256
To link to this Article: DOI: 10.1080/00914039608029378
URL: http://dx.doi.org/10.1080/00914039608029378

Intern. J. Polymeric Mater., 1996, Vol. 31, pp. 237–256
Reprints available directly from the publisher
Photocopying permitted by license only

Flame Retardancy of Cellular Polymeric Materials

R. M. ASEEVA and G. E. ZAIKOV

Institute of Chemical Physics, Russian Academy of Sciences, 4, Kosygin Str., 117334, Moscow, Russia

(Received March 12, 1995)

The combustion behavior of cellular polymeric materials is reviewed. The correlations between the structure and thermophysical properties of cellular polymers are discussed. The tests for potential fire hazard of cellular polymeric materials are reviewed. The approaches to flame retardancy of rigid foams based on reactive polyfunctional oligomers (phenolformaldehyde and urea formaldehyde ones, polyurethane) are demonstrated.

KEY WORDS Cellular polymer, foam, flammability, flame retardancy

1. INTRODUCTION

Cellular polymeric materials (CPM) are notable for the unique combination of technically valuable properties. With relatively small weight they have sufficiently high strength and are characterized by thermal insulating or sound absorbing properties. The filtration potential, selective permeability and the ability to resist large temperature changes are additional interesting characteristics of CPM.

The present volume of world production and the consumption of CPM represents about 10% of the entire plastic production.[1] However, in industrial countries, the part of CPM reaches some polymers such as polyurethanes 50–80%.[2]

In 1990 the volume of CPM consumption by Russian building industry alone was over 5 million m^3. However, at present time the considerable decrease of the production of all types of plastics is noted because of political and economical crisis, that followed the partition of USSR into a number of new independent states.

The importance of CPM for Russia is best demonstrated by use of CPM in heat ducts. About 200,000 km of heatnets with pipes of diameter up to 600 mm and about 20,000 km of pipe lines with diameter of 600–1400 mm are in use in Russia. The quantity of heat energy transported by these systems, is over 9.6 billion GJ/year, which is about 70% of the total consumption of this type of energy.

The heat losses reach up to 10% of the transported energy, and the estimated heat losses of transported energy in 1984 corresponded to about 60 million tons of conventional fuel.

The cellular polymers are usually flammable. Conflagrations cause great and sometimes irreplacable damage. According to data of the World Centre of Fire Statistics the losses from fires in 1977–1980 amounted to 0.4 to 0.8% of national budgets for different countries.[3] In 1982–1983, however, the losses were only 0.1 to 0.48%.[4] This decrease of the damage reflects the measures for prevention of fires. The objective estimation of fire hazard of materials, development of nontoxic flame retardant and low smoke generation systems are the key tasks of fire hazard technology. Due to specific structure features of the heterophasic polymeric CPMs differ because of their specific structure in many respects from their monolithic nonfoamed counterparts.[5-7] Although the chemical composition of CPM plays an important role in the CPM fire hazard characteristics, the physical and morphological structure of CPM also affect the nature of the combustion process.

In the present paper the combustion behavior of CPM is reviewed. The correlations between the structure and thermal properties of cellular polymers are discussed and the tests for potential fire hazard estimation of CPM are reviewed. The rigid foams based on reactive polyfunctional olygomers (of phenol formaldehyde-, urea formaldehyde-type, and polyurethanes) were the main objects of the study.

2. ON STRUCTURAL FEATURES AND SOME PROPERTIES OF CELLULAR POLYMERS

Cellular polymers can be considered as composite materials, containing as filler air or another gas. Gas inclusions impart to polymers a combination of properties, inherent to both the polymer and filling gas.

It is the practice to classify the cellular polymers into foams and porous plastics depending on the geometrical characteristics of gas inclusions, namely whether the gas inclusions are isolated or connected (or closed or open). However, very often the cellular polymers produced have a mixed structure, with a definite ratio of closed and opened cells. The technology of other types of gas filled polymers has also been developed, such as structural foams and multilayer (laminate) foams. CPMs can also be produced as foamed films or foamed fibres.

According to modern conceptions[5-7] the structure of different cellular polymers which fully defines their properties, includes 6 levels of organization[5-7]: 1—molecular chemical structure of polymer; 2—conformational structure of macromolecules; 3—submolecular structure of polymer matrix; 4—spacial structure of gas cells and polymer matrix in the intercellular space; 5—structure and location of microcells in the walls; 6—subcellular structure, characterizing the distribution of gas structural elements in the bulk of the material.

The first and second of the above organization levels of CPM are responsible for all chemical processes of matrix transformation into combusion products. Morphological structure organization levels define macroscopic properties of CPM including their reaction to flame and exposure to high temperatures encountered in fires.

The key to CPM fire safety lies in the understanding of the relationship between chemical and morphological factors and macroscopic properties of gas-filled polymers, especially those, influencing the heat and mass transfer.

The concept of "gas-structural element" suggested by A. A. Berlin and F. A. Shutov[5] allows a quantitative description of CPM morphological structure. The gas-structural element consists of a gas cavity, walls, ribs, and connecting parts. This spacial element of solid and gas phases is replicated in foam material with a definite period and order, degree of intercellular space, etc creating, thus the macrostructure of material.

For quantitative characterizing of CPM macrostructure a number of parameters are being used. They are: apparent density (bulk weight); porosity; number and ratio of open and closed cells; form, size and cell distribution by size and form; the distribution of polymer matrix in walls and struts; surface characteristic, etc.

Porosity, Φ, is defined by the ratio of volume, occupied by gas pores (cells), V_g, and a total volume of system, V_g: $\Phi = V_g/V_0$. The relative gas volume in the foam could be defined as:

$$V_g = 100(\rho_s - \rho)/\rho_s,$$

where ρ_s and ρ are density of nonfoamed polymer and apparent density of CPM, respectively.

CPMs are also characterized by the distribution of apparent density through the volume of CPM. For CPM, consisting of polymer matrix and gas, the volume fraction of polymer, v_s, and gas, v_g, are:

$$v_s = \rho/\rho_s; \quad v_g = 1 - v_s.$$

A large number of structural forms with different gas-structural element position can have an equal value of porosity.

Depending on the manufacturing conditions the CPMs contain isolated and interconnected cells in a defined proportion. Optical and scanning electron microscopy are usually used for structural investigations of CPM. However, the accurate determination of the open cell content is rather complicated due to the planar nature of pictures. That is why sorptional methods are preferred in practice, such as the moisture absorption or volumetric displacement methods.[8]

The idealized forms (monodispersed spheres, hexagons, rhombic dodecahedrons, stretched pentagonal dodecahedrons, capillaries, etc.) were suggested as models for the morphological structure of gas filled polymers.[9] The deviations from such idealized structure are noted with anisotropic forms, obtained by "directional" foaming.

Sizes of cells and their distribution in foamed structure are estimated by statistical treatment of data obtained with the help of conventional methods of structural investigations.

F. A. Shutov[5,6,10] was the first to find a bimodal distribution of cell sizes in the structure of rigid foams based on reactive olygomers (Figure 1). Two types of cells are present in the structure of these CPMs. They are micro and macrocells with sizes of 0.5–1 μm and 60–70 μm respectively. Microcells present the main portion (up to 99%) of total number of cells. However, the contribution of microcells to the general porosity is rather small: about 5–10%.

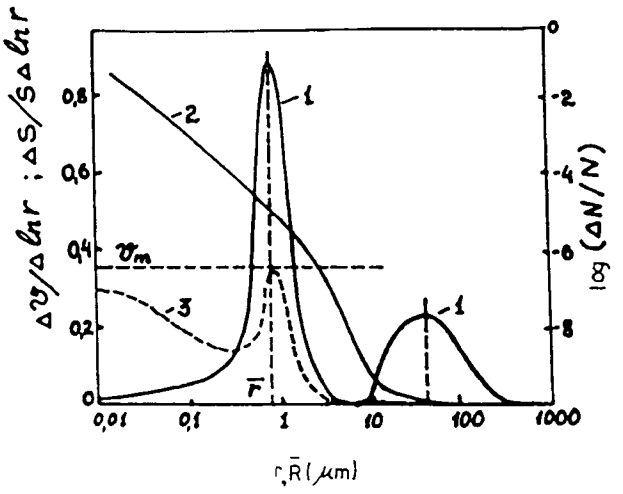

FIGURE 1 The bimodal cell structure of rigid foams based on reactive oligomers: 1—differential distribution of micro and macrocells depending on sizes ($\Delta V/\Delta lnr$); 2—distribution of relative number of cells (lg $\Delta N_i/N$); 3—distribution of specific surface ($\Delta S/S\Delta lnN$).

Unlike macrocells, the microcells have spheric form. They can be isolated or connected. Microcells are located in struts and cell walls. The calculations showed that the thickness of macrocell walls is usually two orders of magnitude lower than their diameter. The maximum thickness of microcell walls, however, is nearly equal to their radius. The linear sizes of microcells are practically independent on the apparent density of CPM.

Large specific surface, both by volume, S_v, and mass, $S_m(S_m = S_v/\rho)$, is another important feature of CPM with a bimodal distribution of cell sizes. The specific surface of rigid foams can exceed 100 m^2/g. For CPM based on reactive olygomers, the microcell formation mechanism is connected with the formation of a three-dimensional network polymer structure on foaming. It is possible to regulate the macro- and microcell structure of foams and their properties by varying the temperature-time cycles of foaming and polymer matrix hardening. The characteristics of polymer distribution in gas-structural elements of CPM affect both the transport and mechanical properties of foams.[11]

Let us consider the heat transfer in CPM. The mechanism of heat transfer includes: the thermal conductivity through solid and gas, the convection through gas phase, and radiation. Considering these components independently, the CPM thermal conductivity can be presented as:

$$\lambda = \lambda_s + \lambda_g + \lambda_c + \lambda_r$$

For a large number of CPM with porosity up to 97%, the volume content of solid phase is small. Nevertheless, this part cannot be ignored because the thermal conductivity of polymer matrix exceeds that of gas in the cells. Nonuniform polymer distribution in gas-structural elements and their anisotropy stipulate different contribution of heat transfer through foam in longitudinal and perpendicular directions.[12] The gas in open cells is the main contributor to heat transfer in foams. For

CPM with closed cellular structure, the gas used as a blowing agent is the main component of gas phase. In open cell CPM, the gas phase consists of air.

Thermal conductivity of gas phase in CPM, having both types of cells, can be calculated by the equation:

$$\lambda_g = \nu_{cl}\lambda_{mix} + (1 - \nu_{cl})\lambda_{air}$$

where ν_{cl} is the volume fraction of closed cells; λ_{mix} is the thermal conductivity of gas mixture in closed cells; λ_{air} is the thermal conductivity of air. The thermal conductivity of a mixture of two gases (for example, freon and air) equals $\lambda_{mix} = \lambda_1^{\nu_1}\lambda_2^{\nu_2}$, where ν_1 and ν_2 are the mole parts of gases. It is known that the thermal conductivity of gas decreases with its molecular mass.

The contribution of convection to heat transfer through CPM becomes noticeable at average cell diameter of 4 mm and higher.[13] This contribution is very small for natural convection and is usually neglected. However, for porous solids with high gas permeability (in presence of filtrational flows) one should not neglect the conventional contribution. It is given by the thermal conductivity of gas and an empyrical fluid dynamic parameter[14]:

$$\lambda_c = 1 \cdot 10^{-2}\lambda_g Re_{eff}; \quad Re_{eff} = V_f d_{eff}/\nu$$

where Re_{eff} is Reynolds number; V_f is gas flow rate; d_{eff} is effective pore size; ν is kinematic gas viscosity.

Let us now consider the heat transfer through CPM by radiation. The radiation contribution can be noticeable. The equation for calculation of radiation contribution to CPM heat transfer assuming that all the polymer is located in the cell walls is given by[15]:

$$\lambda_r = 4\sigma\bar{T}^3 L/[1 + (L/L_g)(1/T_N - 1)]$$

where T_N is the portion of radiation energy transmitted through the cell wall; $\bar{T}$ is average temperature of layer; σ is Stephan-Boltsmann constant; L and L_g are wall thickness and cell size.

T_N can be estimated from the properties of polymer matrix:

$$T_N = (1 - r)/(1 - 2t)][\{(1 - r)t/(1 + 2t)\} + (1 - t)/2],$$

where r and t are coefficients of reflection and transmission of radiation energy of the polymer.

A more accurate estimation of radiation contribution in heat transfer accounting for the distribution of polymer matrix in struts and tangles of cells was suggested in Reference 6.

The effective thermal conductivity of CPM with a closed cellular structure (for example, PU foams including dodecahedron elements) is given by the relationship:

$$\lambda = \lambda_g[(2/3) - \nu_{s,t}/3] + (1 - \Phi)\lambda_s + 16\sigma\bar{T}^3 l_r/3K$$

The equation reflects the contributions to heat transfer by conduction through gas and solid phases of CPM and by radiation. K represents average extinction coefficient of grey solids in UV region of spectrum, $v_{s,t}$ is the volume fraction of polymer in the struts. Accepted numeral coefficients assume that 1/3 of struts is oriented in the heat flow direction.

The analysis of factors, which lead to a decrease of all components of heat transfer, led to development of PU foams with a very low effective thermal conductivity (0.014–0.015 W/m·K).[17]

The influence of apparent density on thermophysical properties of foams based on reactive olygomers are described by the following regression equations[18] obtained for phenolic foams with ρ of 40–1200 kg/m^3: $\lambda = 2.85 \cdot 10^{-2} + 1.84 \cdot 10^{-4}$ ρ, W/m·K; thermal diffusivity $a = (240/\rho) + 0.7$; $(a \cdot 10^7)$, m^2/s. For polyurethane foams with ρ to 325 kg/m^3: $\lambda = 2.85 \cdot 10^{-2} + 0.85 \cdot 10^{-4}\rho$; $a = (218/\rho) + 0.3$; $(a \cdot 10^7)$, m^2/s. If the apparent density ρ, volume portion of open cell v_{open}, and volume portion of closed cell with freon v_{fr}, are taken into account, the following regression equation for calculation of thermal conductivity is used[19]:

$$\lambda = 34.76 - 0.142\rho - 0.08v_{open} - 0.10v_{fr} + 2.5 \cdot 10^{-3}\rho^2 + 7.3 \cdot 10^{-4}v_{open}^2 + 5 \cdot 10^{-4}\rho v_{open} - 1.5 \cdot 10^{-3}\rho v_{fr} + 1.6 \cdot 10^{-3}v_{open}v_{fr};\ \text{mW/m} \cdot \text{K}$$

3. FIRE HAZARD TESTING OF CELLULAR POLYMERIC MATERIALS

There is a large number of tests to study flammability and fire hazard of CPM. The test methods are divided into bench-scale size (to 120 cm), large-scale size (above 120 cm) and real item testing.[20] Although there are some difficulties in relating the results of bench-scale flammability tests with real fire behaviour for CPM, small and middle-scale tests continue to be of value for many investigation purposes.

Some of the bench-scale methods for fire hazard testing of polymeric materials used in Russia, correspond to state standard of GOST 12.01-44-89.[21] The standard includes the methods for the estimation of ignitability indices, flame spread, gas toxicity and smoke formation at combustion or pyrolysis of polymeric materials. In the present work the following tests were used in accordance with GOST 12.01-44-84: the limiting oxygen index (corresponding to ISO 4589); the ignition and self-ignition temperatures (analogous to ASTM D 1929); the flame spread index and ceramic tube index (CT index).

CT index represents the ratio of the heat released as a result of polymer combustion to the heat required for the sample ignition. At CT index values of less than 1, the materials are considered hard combustible. At CT index of more than 1, the materials are combustible. Among the combustible ones the group of hard ignitable polymer materials is detected with CT indices in ranges from 1 to 2.5. Foam samples have sizes of 150 × 60 × (to 30) mm.

The flame spread index, I, is determined for samples with sizes of 320 × 140 × δ (to 20) mm. The sample is placed at 30° angle to the radiant panel, that

TABLE I

Fire hazard indices of some industrial CPM produced in Russia

CPM type	ρ, kg/m³	Fire hazard indices: LOI %	Fire hazard indices: CT, Index	Fire hazard indices: I	Smoke form, D_{max}^{m}	Toxicity, H_{CL-50}, g/m³	T_{ign}, °C	T_{si}, °C
Phenolic PhRP-1	40 – 120	34 – 40	0.6 – 2.2	<20	14 – 19* 4.5 – 5.5†	6.6 – 14* 210*†	470 – 500	540 – 600
Urea formald.								
MPhP-3	15 – 30	30 – 34	1.3	<20	110 – 250*	—	300	475
PKZ-30	25	34	1.35	<20	200*	—	280 – 300	450 – 475
Polyurethane foam						24 – 29.2*		
PPU-316M	50 – 180	20 – 22.5	1.9 – 4.5	29.8	520 – 845†		360	530

*Pyrolysis conditions, † Combustion ones. Critical heat flow for PhRP-1 ignition is 30.4 kW/m² (for foam with ρ = 50 kg/m³). Effect of CPM porosity on LOI is insignificant.

provides heat flow from 3.3 W/cm^2 to 1.25 W/cm^2 over the sample length. A pilot flame (3.1 kJ/s) is used for ignition. The flame spread index is calculated using:

$$I = \left[0.0115\beta\{(T_{max} - T_0)/\tau_0\} \left\{ 1 + 0.21 \sum_{i=1}^{n} (l/\tau_i) \right\} \right]^{0.5}$$

where β is thermal constant of apparatus; τ_0 and τ_i are times of flame front reaching the zero and ith marks; l is the distance passed by the flame front; T_{max} and T_0 are maximum and initial temperatures of released gases. The materials are subdivided into 3 groups by flame spread: nonspreading ($I = 0$), slowly—(I up to 20) and fast spreading ($I > 20$).

The smoke formation ability of CPM has been determined by the standard method of GOST 24632-81 (corresponds to ISO 5659).

Pyrolythic gas chromatography and mass-spectroscopy have been used for analysis of gaseous products of polymer decomposition in the temperature interval between 300–800°C. Apparatus of GCh-5CO_2-2 type was used also for fast analysis of CPM combustion products.[21] Table I shows the examples of fire hazard characteristics of some industrial CPM based on reactive olygomers.

Phenolic and urea formaldehyde foams are hardly ignitable ones. Phenolic foams of PhRP-1 type are hardly combustible, if their apparent density exceeds 80 kg/m^3. These foams show very low optical density of smoke. However, high toxicity of combustion products is one of the disadvantages of the phenolic foams.

4. FLAME SPREAD ALONG THE SURFACE OF CELLULAR POLYMERS

The phenomenon of flame spread along the surface of various combustible materials has been studied to a considerable extent both experimentally and theoretically. The flame spread (FS) is a result of complex interactions of mass and heat transfer processes and chemical reactions in gas and condensed phases. The rate of combustion wave propagation is considered the main FS index.

The fundamental FS investigations elucidated the mechanisms controlling the process. Two main mechanisms have been clarified depending on conditions of FS characteristics, the heat transfer from the flame to ignited surface of material and the kinetics of gas phase chemical reaction of fuel vapors with oxidizer.

Numerous FS types are usually classified by spacial orientation of the material, direction of combustion wave and oxidizer flow, combustion hydrodynamics and thermal thickness of the sample. The reviews of studies concerned with FS modes are given in References 22–24. Most of the theoretical FS models are thermal, as they describe heat transfer to the surface of combustible material both from its own flame and external source. Heat transfer from the flame to the material surface occurs by heat conductivity or convection through the gas phase, heat conductivity through a condensed phase and by radiation from the flame.

To calculate the FS rate, V_{fs} we assume that the heat flow, $\dot{q}''$, to inflammable material is used to change the material enthalpy, ΔH, necessary for ignition[25]:

$\rho V_{fs}\Delta H\delta = \dot{q}''l$, where ρ is the fuel density; δ is the thickness of pyrolyzable layer; l is the surface area affected by heat flow from the flame.

The determination of predominant mode of heat transfer helps us to understand the main regularities of FS along the material surface. Various external factors, affecting heat transfer from the reaction zone to the surface, affect the FS rate. External radiation heat, changes in temperature of material and surrounding, the heat loss from the article, oxygen concentration in oxidizer flow, the flow rate of latter, pressure, etc., are among these factors.

The direction of gaseous oxidizer flow in respect to the combustion wave influences the FS rate as it usually weakens (at opposed flow) or increases (at concurrent one) the heat transfer from the flame to the surface. Both modes of flame spread can be presented as pyrolysis front spread (x_p) and described by the same approximate functional equations. For example, for thermally thick materials we have[26]:

$$V_{fs} = dx_p/d\tau = \dot{q}_f''^2 l_f/(T_i - T_s)^2\lambda\rho c$$

where $\dot{q}_f''$ is the heat flow from the flame to the surface at the distance l_f before pyrolysis front; x_p is pyrolysis front coordinate; T_i is the ignition temperature; T_s is the surface temperature at the l_f distance. If the directions of the oxidizer flow and of the flame, are opposite $\dot{q}_f''$ and l_f depend largely on thermal properties of the material. FS rate at concurrent oxidizer flow depends to a great extent on the heat release rate, which is related to the burning mass rate of material.

At concurrent flow of gaseous oxidizer and flame movement, the FS rate increases. The analysis of FS of this mode predicts the power dependence of FS rate on time and pyrolysis zone length of the material. CPMs differ from related monolithic materials in density, and thermal and physical properties. The decrease of thermal inertia ($\lambda\rho c$) for CPM should increase the FS rate according to the above mentioned equation.

In this work the characteristics of the downward laminar diffusion FS over PU foam slab are determined using the LOI test apparatus. It was interesting to study the effect of porous foam structure (apparent density) and of other factors on the FS rate. To elucidate the mechanism of heat transfer from the flame creeping to inflammable PU surface, the temperature profiles near the leading edge of the flame are examined in detail. Pt-PtRh thermocouples with noncatalytic coating are used. A microdevice positioned the thermocouples at 0.25 mm intervals normal to the vertical surface. The temperature-time (distance) data are recorded by H115 oscillograph. Figure 2 shows the temperature distribution profiles obtained for the steady downward flame spread along vertical slab of PU foam having $\rho = 49$ kg/m^3 at $Y_{O_2} = 0.26$.

The foam samples of size of 1.25 × 1.25 × 15 cm behave like the thick samples do. At the condition studied the thickness of the surface porous layer heated under the flame leading edge is equal to 1.1 mm. The surface temperature is 648 K. The flame leading edge is located 1.5 mm above the PU foam surface. The maximum flame temperature is 1220–1370 K.

The temperature data are used to calculate the energy balance for the condensed

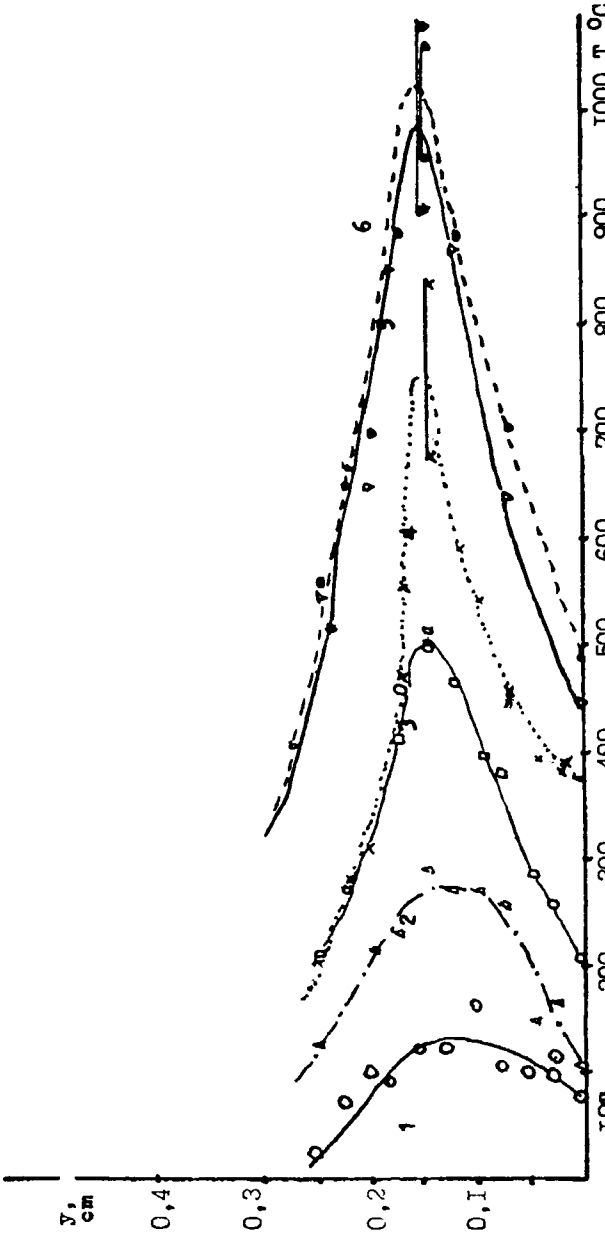

FIGURE 2 Temperature distribution profiles in the gaseous phase at downward flame spread along PU foam sample (ρ = 49 kg/m^3) 1. x = 2; 2. x = −1; 3. x = −0.5; 4. x = 0; 5. x = +1; 6. x = +1.5 mm.

phase. For the laminar flame spread over small samples size PU foams the heat feedback, $\dot{q}''_s$, from the flame to the inflammable surface is consumed to raises the temperature of the layer, $\dot{q}''_h$, and pyrolyze the fuel, $\dot{q}''_s$: $\dot{q}''_s = \dot{q}''_h + \dot{q}''_{pyr}$.

For the steady process at $x < 0$, $\dot{q}''_s = \dot{q}''_h$. The net flux of thermal enthalpy is $\dot{q}''_h = \delta_{cy}\rho V_{fs} c(T - T_0)$, where δ_{cy} is the thickness of porous layer heated; c is the heat capacity of foam. In the case considered the heat transfer mechanism includes gas and solid phase thermal conduction through the cellular surface layer with depth of δ_{cy}. From the experimental data on flame spread rate, the temperature distribution profiles and temperature gradients in gas and solid phases the values of $\dot{q}''_h$, $\dot{q}''_g$, $\dot{q}''_{cs}$ are calculated separately as function of distance x.

The data in Figure 3 show that near the leading flame edge a considerable fraction of heat transfer from flame is by thermal conduction through the porous layer (about 30–40% of the net heat flux from flame). At $x \geq 1$ mm the heat transfer through gas phase becomes the dominant mechanism of the flame spread along the PU foam surface in this small scale test.

We found that the surface and flame temperatures increase to 675–680 K and to 1350–1450 K when oxygen content into oxidizer flow increases to 28%. The thickness of the heated surface cellular layer is reduced to 0.8 mm. Due to low thermal inertia of PU foam the heat transferred from flame to the inflammable surface of cellular body is accumulated in this thin surface layer.

The mechanism of flame spread over a charring PhRP-1 phenolic foam with density of 60 Kg/m^3, exposed to 40°C during 10 hours, was studied. The rate of

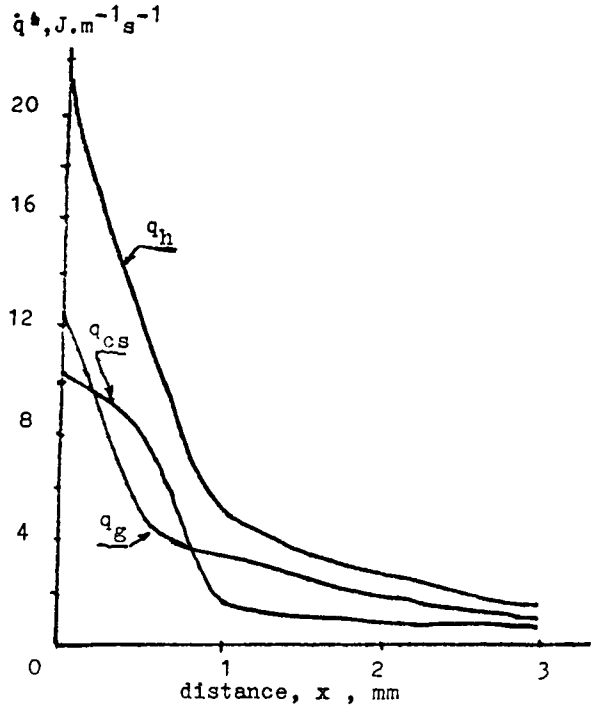

FIGURE 3 Heat fluxes distribution ahead flame front at downward flame spread along PU foam.

downward flame spread over the foam surface at oxygen content in oxydizer flux of 50% was 0.3 mm/s. The surface temperature under flame leading edge was 740–768 K. Maximum surface temperature of carbonized layer (1170 K) was reached at a distance of 0.56 mm from the flame leading edge. By using the temperature profiles in the combustion front, the thermal balance was calculated. We found that in this small-scale test the heat transfer by the thermal conduction through gas phase is the dominant mechanism of flame spread over charring foam. The heat transfer from the flame by radiation is insignificant (<1% of net heat flux to the surface). The radiation from the incandescent char is more important for the heating of surface layer under flame leading edge. Ahead of flame edge, however this mode of heat transfer has no role.

It should be noted that maximum flame temperature at flame quenching limit for all used foams does not exceed 1370 K.

In the present work it is found that the flame spread velocity depends on apparent density of foams. In a general form this dependence is described by the equation:

$$V_{fs} = K\rho^{-n}$$

where K and n are constants.

Table II shows the experimental results, obtained for the flame spread over PU and phenolic foams in the downward vertical directions.[27] The results observed show that the chemical nature of cellular polymers and their apparent density affect the flame spread rate.

The results obtained for rigid PU foams can be described by equation:

$$V_{fs} = 2.8 \times 10^2\rho^{-1.1}, \text{ mm/s.}$$

For the phenolic foams we have the following correlation:

$$V_{fs} = 0.636 \times 10^2\rho^{-1.15}, \text{ mm/s.}$$

It should be noted that the flame spread rate over the foam surface in horizontal direction was practically the same as the one in the downward vertical direction. The value of "n" in above equations almost reaches its theoretical value one. Thus,

TABLE II

The effect of apparent density of rigid foams on FS rate

	Apparent density, kg/m³								
PU foam	30.9	31.2	33.5	34.6	47.6	48	48.8	74	77.8
V_{fs}, mm/s (Y_{ox} = 0.265)	7.4	7.36	5.45	4.93	3.84	3.7	3.26	2.8	2.6
	Apparent density, kg/m³								
Phenolic foam (Y_{ox} = 0.43)	31.8		49.3		60		81.3		120
V_{fs}, mm/s	1.2		0.70		0.57		0.41		0.26

the cellular polymers of low apparent density can develop a higher rate of flame spread. A large effect of thermal inertia of cellular polymers on FS rate may be illustrated by comparing two rigid PU foams with roughly equal density (49 and 40 kg/m^3) and porosity (96.1 and 96.6%) but with different values of thermal inertia ($\lambda\rho c \cdot 10^{-3}$ are 2.3 and 1.78, W^{2}s/m^{4}K^2). The FS rate along surface of PU foam with lower thermal inertia is almost twice as high as the FS rate with higher thermal inertia foam.

The oxygen content in the oxydizer flux (O_2 + N_2) has a considerable effect on the flame spread rate over cellular polymers. The effect is increased when the apparent density of foam is decreased. For example, the dependence of the FS rate over PU foam having ρ = 49 Kg/m^3 on oxygen content in limits from 25 to 30% vol. is approximated by the equation:

$$V_{fs} = 3.7 \times 10^5 Y_{ox}^{8.5} \text{ mm/s.}$$

For PU foam with ρ = 70 kg/m^3 the dependence corresponds to:

$$V_{fs} = 3.4 \times 10^4 Y_{ox}^{7.4} \text{ mm/s.}$$

5. FLAME RETARDANCY OF RIGID FOAMS BASED ON A REACTIVE OLYGOMERS

The important feature of rigid foams based on a reactive olygomers is the presence of the stage of polymer network formation and the formation of cellular macrostructure in one technological cycle. Therefore, one of general requirements to flame retardants used for the production of the rigid foams is absence of negative effects on chemical reactions of network formation and foaming.

5.1 Phenolic Foams

Phenolformaldehyde foams are widely used as thermal insulation materials in building industry. At relatively low apparent density (40–80 kg/m^3) they are characterized by low values of thermal conductivity, high heat resistance and structural stability. These foams are hardly ignitable materials with low smoke formation. However, phenolic foams have the number of serious shortcomings: low mechanical strength, corrosive activity, unsufficiently high thermooxidative stability, the inclination to smouldering and also high toxicity of combustion and pyrolysis products.

The objects of present study are phenolic foams of liquid type based on cold hardening resol phenolformaldehyde olygomers. For the production of flame retardant phenolic foams the components of industrial rigid foams of PhRP-1 type are used: for example, the phenolformaldehyde resin of PhRV-1A type (Technical grade 6-06-1104-78) and the foaming and hardening agent of VAG-3 type (Technical grade 6-05-116-78).

PhRV-1A resin is a mixture of resolic phenolformaldehyde olygomers with aluminium powder and a surface-active substance OP-10. The foaming and hard-

ening agent VAG-3 is a condensation product of sulphophenylcarbamide with formaldehyde and ortho-phosphoric acid. The typical formulations of the compositions for production of phenolic foams consist of 100 mass. parts of PhRV-1A and 15–25 mass. parts of VAG-3. Foaming is the result of hydrogen formation on the action of acid with the aluminium powder.

The purpose of the present work was to obtain the flame retardant phenolic foams with improved performances. The following approaches were carried out: a) the use of reactive phosphorus-containing substances, which lead to formation of polymer matrix with interpermeated or semi-interpermeated network structure (network-network or network-linear polymer), and b) the use of the additives with multifunctional mechanism of the action, which affect different characteristics of the initial composition and of the foam.

We investigated the bis(2-chloroethyl)1-bromovynilphosphonate(bromophos-1) and bis(2-hydroxyethyl)methacrylphosphonate (PhEM) as reactive flame retar-

TABLE III

The properties of flame retardant phenolic foams[28–31]

Indices	Phosphorus containing flame retardant			
	PhEM	Bromophos-1	Phosphopolyol	PPhPh
FR content, pph by weight	3.3–16.7	2.4–14.8	7.0–10.5	1–10
Apparent density, kg/m^3	65–56	45–65	58–114	60–85
Compressive strength, kPa	150–230	100–230	110–310	115–230
Water absorption during 24 h, %	12–16	14–20	12–18	14–29
Heat resistance, °C	170–175	160–165	170–175	165–170
Acid number, mg KOH/g	—	—	2.8–8.7	—
Decomposition temperature, °C	280–300	265–275	280–300	280–300
Mass losses, % (fire tube test)	12.8–14.2	10.0–15.4	11.4–16.0	10–16
CT index	0.2–0.47	0.17–0.37	0.15–0.21	—
LOI, % vol.	41.7–45.0	35.4–49.5	48.5–58	42.4–48.3
Smouldering temperature, °C	—	—	300–320	300–310

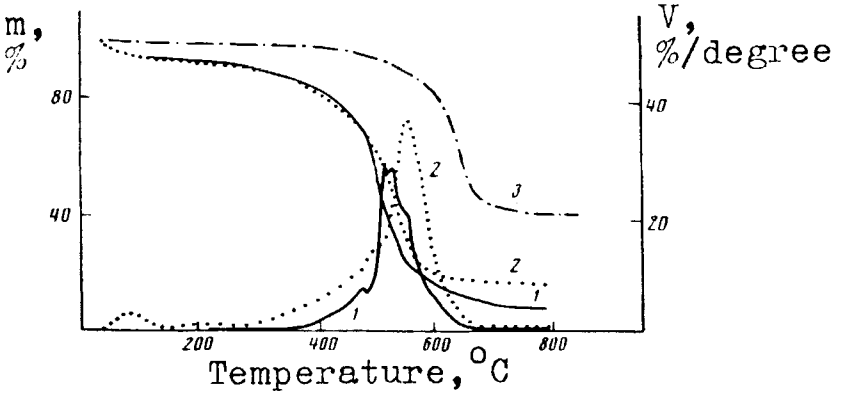

FIGURE 4 TG and DTG curves of decomposition for phenolic foam (1), phenolic foam with 10% PPhPh (2) and PPhPh (3).

dants. The substances are well compatible with PhRV-1 resin. They affect neither the foaming nor the hardening stages of the process. The obtained foams have a homogeneous, small cellular structure. Table III shows the properties of modified phenolic foams. The results for the modification of PhRP-1 foam with poly(1,4-phenylenephenylphosphonate (PPhPh) are also given. PPhPh (Rhone-Poulenc product) is a linear polymer with $\bar{M}_n$ = 10000–11500. PPhPh thermal decomposition is above 375°C (Figure 4). The additive behaves as a disperse filler in the resin which leads to a small increase of the foam apparent density on addition of PPhPh.

The modified phenolic foams are hardly combustible, no smouldering is observed after the removal of flame. When phosphorus content in the foams reaches 0.8–1% mass the critical thermal flux of ignition increase to 45–50 kW/m^2. The mechanical strength of modified foams is higher than that of control foams. The air temperature, above which a steady smouldering for foams ignited by pilot flame appears, is also higher (310–320°C) than that of the control (250–270°C).

The comprehensive study of thermal decomposition of phenolic foam modified by PPhPh is reported in Reference 31. It was determined that PPhPh affects the content of volatile products and char yield (Table IV). The balance of volatile amounts confirms that at high temperature pyrolysis all phosphorus of PPhPh of phenolic foam remains in the condensed phase. The flame retardancy mechanism of phenolic foams by PPhPh is attributed to the increase in char yield, the formation of surface polyphosphate layer at pyrolysis of cellular polymer and the retardation of thermooxidation of carbonized residue.

Industrial resins, used for phenolic foam production, contain the light volatile toxic compounds such as free phenol (to 9%) and formaldehyde (to 3.5%). During foaming and hardening of foam composition high temperatures (to 110°C) are developed as result of exothermal reactions. The toxic compounds volatilize and produce hazardous working conditions.

It was shown that the application of small amounts (0.02–2 pph) of metal halides

TABLE IV

The PPhPh effect on the composition of thermal degradation products of phenolic foam[31]

Product	Content, % weight, at temperature, °C				
	300°	400°	500°	600°	700°
CO	0.07/0.03	0.08/0.08	2.7/1.3	3.9/4.6	4.0/3.8
CO_2	0.1/0.07	0.29/0.13	3.1/2.8	4.2/3.1	3.5/2.2
CH_4	0.2/0.14	0.25/0.27	4.0/2.3	5.2/4.5	5.9/6.7
H_2O	0.87/0.2	0.91/0.66	4.1/4.0	5.9/7.5	6.6/7.5
CH_2O	0.06/0.04	0.44/0.25	1.0/1.24	1.1/1.9	0.8/1.7
Benzene	1.0/0.6	2.0/1.6	5.3/9.8	9.9/12.1	17/21.4
Toluene	—/trace	—/trace	2.3/4.5	2.0/3.8	4.1/2.0
Phenol	4.6/3.8	16.9/11.2	34.6/29.7	45.9/48.2	48/47.1
o,m,p-cresols	—/trace	—/trace	trace/2.4	trace/3.1	—/0.5
Fraction with T_{vol} > 200°	92.3/95.1	78.8/85.8	47.0/42	21.9/11.2	9.4/7.4
Nonvolatile residue	87.2	82.5	56.9	37.5	36.8

Numerator—without, denominator—with 10% PPhPh; 2 min. isothermal heating in inert atmosphere.

or metal borohalides, such as AlF_3, $SnCl_2 \cdot 2H_2O$, $Zn(BF_4)_2 \cdot 6H_2O$ permits to decrease the apparent density of foams, the content of free phenol in the articles and also to use a unconditional resins after long keeping.[32,33] The formation of metal salt complexes with phenol has been shown by UV-spectroscopic analysis of model systems including phenol.

The complexing activity of salts decreases in the following order:

$$SnCl_2 > Zn(BF_4)_2 \geq AlF_4 > CuF_2 \geq MnCl_2 \approx Ni(BF_4)_2 > NiCl_2$$

At introduction of 0.02–0.05 pph AlF_3 the apparent density of foams obtained in comparison with foam without additive decreases from 51 to 45.3–38 kg/m^3, however, LOI increases from 37.7 to 40.3–41.5%. The compression strength of foams remains on the level of 135–140 kPa, and a considerable decrease of free phenol content in foam is observed.[32]

The addition of salts permit us to obtain phenolic foams with good performance using resins aged for 6 months. For example, a typical foam formulation, but with the application of PhRV-1 resin exposed at 20–25°C for 6 months, a foam with apparent density of 165 kg/m^3 is produced. The use of AlF_3 additive (2.5 pph) permits us not only to develop phenolic foam with ρ = 75 kg/m^3 but also to decrease the free phenol content from 5 to 1.1%.[32]

The effects observed are connected with the influence of the additives on rheological properties of polymeric composition, on the reactions of hydrogen evolution and polycondensation of resin components. The modified phenolic foams have structures containing in part closed cells.

The flame retardancy of rigid phenolic foams can be improved by using high temperature stabilizers against thermooxidative decomposition of cellular polymer.

It is shown that cupric complex of macroheterocyclic compound is an effective stabilizer for thermooxidative decomposition of phenolic foams at temperature above 200°C. The addition of 0.25–5.0 pph permits to decrease the ignitability of phenolic foams at high temperatures in air environment.[34]

Urea Formaldehyde Foams

The urea formaldehyde foams (UFF) have a more narrow working temperature interval (from −20° to +130°C) than the phenolic foams. The low mechanical strength, high water and moisture absorption, considerable shrinkage, the release of free formaldehyde during production and use are the main shortcomings of UFF. Chemical modification of UFF and the use of inorganic phosphorus and nitrogen-containing flame retardants are the general approaches to UFF flame retardancy. Hardly combustible UFF's with closed cellular structure are developed by chemical modification and addition of 1–2 pph of phosphorus containing substances.[35] At flame retardant content above 2–2.5 pph the strong increase of times for the beginning and the termination of foaming process is observed.

The UFFs developed (ρ = 60–120 kg/m^3) have the following flammability indices: LOI is 40–41%; ignition and self-ignition temperature are 285–305° and 465–475°C respectively; CT index is 0.31–0.55. A great deal of work was done to decrease the formaldehyde offgassing during the UFF production.

We suggested that on strengthening of intermolecular interaction the formaldehyde will first retain its associated state and only gradually participate in the network formation process. The preliminary results based on this hypothesis are promising.

Rigid Polyurethane Foams

The thermal insulation materials based on rigid polyurethane foams (PUF) are the leading cellular polymers used in building and transportation. These cellular polymers are popular because of simple production technology, relatively low cost and high insulation properties.

Reactive and additive flame retardants, containing halogen, phosphorus and nitrogen, have been used extensively in such foams to decrease their flammability. In recent years there has been a growing interest in the development of rigid PUF which perform better in fire tests and conditions. This has led to a general tendency to limit the use of halogen-based flame retardants in spite of their relatively large effectiveness in improving the reaction to fire of polymer materials.

The effect of halogen free reactive flame retardant on the main technological properties and fire safety indices of rigid PUF has been investigated.[36,37]

A starting formulation for producing a rigid PUF modified includes the following components:

	Part by weight
Polyisocyanate (Technic. condit. TC 6-03-296-78)	125
Polyol Laprol 503 or Laprol 805 (TC 6-05-1679-74) } N-containing polyol Lapromol-294 (TC 6-05-1681-74) }	100
Dimethylethanolamine	2
Freon-11 (TC 6-02-727-78)	to 30

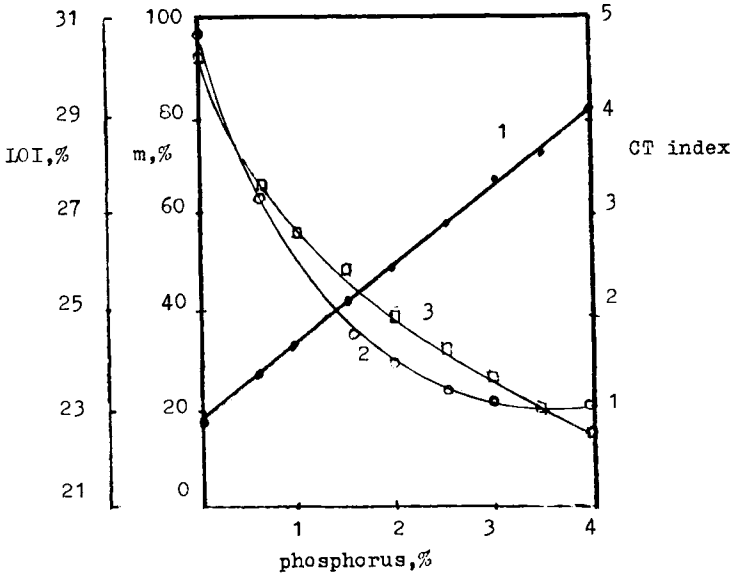

FIGURE 5 The dependence of flammability indices for PU foams on phosphorus contents: 1—LOI; 2—mass losses at fire tube test; 3—CT index.

Phosphorus-containing flame retardant is used in limits of 10–70 parts. Phosphorus-containing olygoester ethoxylated (phospolyol) has viscosity of 18.43 cPa.s at 75°C. It contains of 15.2% P, 0.08% water and 11.0% hydroxyl groups. It is found that phospolyol decreases the start of foaming from 28 to 21 s, and the termination time of foaming from 110 to 70 s (for 70 parts of phospolyol).

Figure 5 shows that the flammability indices of PUF modified depend on phosphorus contents. Optimum *P* contents in foam is about 2.5%. In this case PUF has the following properties:

The apparent density, kg/m^3	50–55
Compressive strength, kPa	340–360
Water absorption for 24 hours, %vol.	1.7–1.8
Thermal conductivity, W/m·K	0.028
Limiting oxygen index, %vol.	27.6–27.8
CT index	1.34–1.4
Smoke optical density D^m_{max} at combustion	237–245
at pyrolysis	103–107

The composition of pyrolysis products of FR foam does not change significantly with the increase of *P* contents (Table V).

TABLE V

The composition of pyrolysis products of rigid FR foam (2.5% P)

Mass loss at 400°C	Contents, %							
	CO	CO_2	H_2O	CH_4	C_2H_6	C_2H_4	C_3H_6	HCN
83.8	0.37 / 2.44	1.8 / 4.69	0.61 / 0.97	0.11 / 1.40	0.06 / 0.17	trace / 0.02	0.22 / 0.31	— / 0.028

Numerator—at 400°, denumerator—at 700°C.

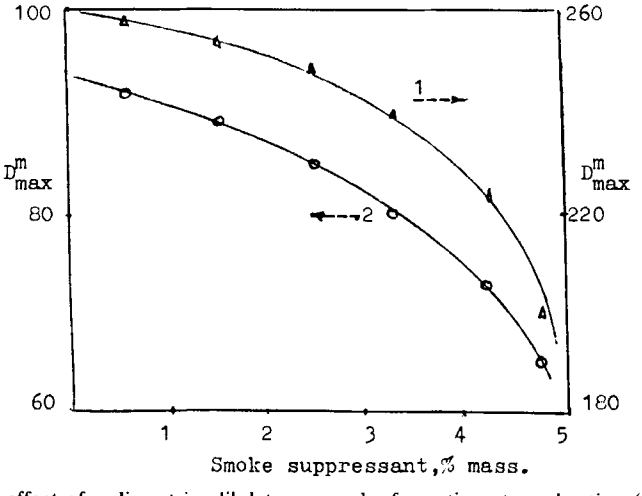

FIGURE 6 The effect of sodium trimolibdate on smoke formation at combustion (1) and pyrolysis (2) of phosphorus containing PU foam.

Thus, the modified PUFs are hardly ignitable materials. Toxicity of high temperature pyrolysis products for PUF is related to the increasing HCN content. To decrease the ability of foam to form smoke it was proposed to add sodium trimolybdate (Figure 6). This compound does not affect LOI of foam, but decreases toxicity of pyrolysis and combustion products. For example, on addition of 2% of smoke depressant, the CO contents decreases from 0.37 to 0.06% vol; the critical heat flow for the PU foam ignition increases from 18.1 (without FR) to 30.5 kW/m^2.

6. CONCLUSION

Some aspects of combustion behavior and flame retardancy of rigid cellular polymers based on reactive polyfunctional olygomers have been considered. The proposed approaches to solve the flame retardancy problem for cellular polymers, permit us to develop high performance rigid phenolic foams, urea formaldehyde and PU foams.

References

1. "Saechtling International Plastics Handbook for Technologist Engineer and User," 2nd Ed., Hanser Verlag, Munchen, 1987.
2. V. N. Felichkina, "Chemical Industry Abroad," 1987, pp. 41, in Russian.
3. *Palontorjunta*, **33**, 560 (1982).
4. *Brandvaern*, **13**, 17 (1987).
5. A. A. Berlin and F. A. Shutov, "Chemistry and Technology of Foamed Polymers," Science, Moscow, 1980, in Russian.
6. A. A. Berlin and F. A. Shutov, "Foamed Polymers Based on Reactionable Olygomers," Chemistry, Moscow, 1978, in Russian.
7. A. A. Berlin and F. A. Shutov, "Structural Foamed Plastics," Chemistry, Moscow, 1980, in Russian.
8. A. Schauer *et al.*, *Stavebnicky casopis*, **15**, 245 (1967).
9. R. H. Harding, Resinography of Cellular Plastics, ASTM Spec. Tachn. Publ. N414, ASTM, Philadelphia, 1967, pp. 3.
10. Yu. M. Tovmasyan, F. A. Shutov *et al.*, *Reports of USSR Academy of Sciences*, **263**, 156 (1982), in Russian.
11. A. A. Berlin, I. I. Chaikin and F. A. Shutov, *Plastmassy*, 14 (1982).
12. A. Gunningham and D. J. Sparrow, *Cellular Polymers*, **5**, 327 (1986).
13. R. E. Scochdopole, *Chem. Eng. Progr.*, **57**, 55 (1961).
14. M. E. Aerov, O. M. Todes and D. A. Norchinsky, "Apparatus with Stationary Grained Layer," Chemistry, Leningrad, 1979, in Russian.
15. R. Williams and C. M. Aldao, *Polym. Eng. Sci.*, **23**, 293 (1983).
16. M. A. Schuetz and L. R. Glicksman, *J. Cell. Plast.*, **20**, 114 (1984).
17. A. Cunningham, G. M. F. Jeffs, *et al.*, *Cellular Polym.*, **7**, 1 (1988).
18. A. D. Golikov and V. M. Ivanov, "Chemistry and Technology of Production Processing and Application of Polyurethanes," Chemistry, Vladimir, 1984, pp. 86, in Russian.
19. A. G. Dementyev, O. G. Tarakanov and M. I. Fedotova, ibid., p. 43.
20. C. J. Hilado, "Flammability Test Method Handbook," Tachnom. Publ., 1973.
21. GOST 12.1.044-89, Fire Hazard of Substances and Materials.
22. I. S. Wichman, *Progr. Eng. Comb. Sci.*, **18**, 553 (1992).
23. *Combustion Sci. Technology*, **32**, 1–209 (1983).
24. A. C. Fernandez-Pello, *Comb. Sci. Techn.*, **39**, 119 (1984).
25. F. A. Williams, 16th Symposium (Intern.) on Combustion, Pittsburgh, Comb. Inst., 1977, pp. 1281.
26. J. Quintiere, *Fire and Materials*, **5**, 52 (1981); **9**, 65 (1985).
27. R. M. Aseeva, L. V. Rubun and L. Zabski, *Intern. J. Pol. Mater.*, **14**, 127 (1990).

28. R. M. Aseeva, V. A. Ushkov, L. V. Ruban, G. E. Zaikov *et al.*, SU author. sert. N825557, Int. Cl³ CO8 J 9/06, SU Bulletin of Inventions 1981.
29. R. M. Aseeva, V. A. Ushkov, L. V. Ruban, G. E. Zaikov *et al.*, SU author. sert. N664436 SU Bul. Inv. 1979.
30. V. A. Ushkov, R. M. Aseeva, R. Andrianov, G. E. Zaikov *et al.*, SU auth. sert. N1407021, 1988.
31. R. M. Aseeva, M. I. Artsis, G. Vivan and G. E. Zaikov, *Vysokomol. soed.*, **29A**, 2596 (1987).
32. R. M. Aseeva, V. A. Ushkov, G. E. Zaicov *et al.*, SU author sert. N872532, SU Bull. Inv. 1981.
33. M. G. Bruyako, R. M. Aseeva, V. A. Ushkov *et al.*, SU author sert. N784303, SU Bull. Inv. 1980.
34. F. A. Shutov, R. M. Aseeva, V. V. Ivanov *et al.*, SU author sert. N535323, SU Bull. Inv. 1976.
35. V. A. Ushkov, O. V. Zacharova, V. V. Samoshin *et al.*, *Plastmassy*, 72 (1989).
36. V. A. Ushkov, R. M. Aseeva, V. I. Kalinin *et al.*, Plastmassy, 21 (1984).
37. V. A. Ushkov, R. M. Aseeva, V. N. Vorobyev *et al.*, Plastmassy, 45 (1989).